OG 1228

BNL-61315

Conf-9409268--4

Performance of an Accordion Electromagnetic Calorimeter with Liquid Krypton

David Lissuaer
Brookhaven National Laboratory Address
Upton, New-York 11973, USA
E-mail: Lissauer@bnl.gov

ABSTRACT

Beam test results of the liquid krypton electromagnetic calorimeter with a projective accordion type electrode structure are presented. The electrode had a fine segmentation in the front to enhance π^0 rejection and pointing. The test was carried out at the H4 line at the CERN SPS with e^- beams between 20 and 200 GeV. Preliminary results of energy resolution, linearity, μ response and the dependence of the energy resolution on the amount of inactive material in front of the calorimeter are presented.

1. Introduction

The physics requirements of the LHC require the development of a fast, stable, finely segmented calorimeter with excellent energy resolution and a small constant term at high energy. For example experiments designed for LHC[1] and SSC[2] to search for the Higgs via its decay into two photons, $H \rightarrow \gamma\gamma$, require very good energy resolution and background rejection. The aim of this test has been: a) to bring the energy resolution of an EM accordion calorimeter[3,4] into the range of about $5.5\%/\sqrt{E}$ with a small constant term; b) to achive good position and pointing resolution by using a finely segmented first section that will act as an integated pre-shower[2] detector; and c) to study the energy resolution dependence on the amount of inactive material in front of the calorimeter.

To improve the energy resolution we have taken an obvious step of increasing the sampling fraction by replacing the liquid argon (LAr) with the next heavier noble liquid, liquid krypton (LKr). Keeping the same volume (i.e. depth) of the calorimeter allows one to achieve a higher sampling frequency and a higher sampling fraction. A non projective acordion has been tested by us at BNL [5,6,7,8]. In this test we have built a projective accordion module with an integrated pre-shower section.

2. Experimetal setup

The test of the calorimeter was conducted at the H4 beam line at the SPS at CERN, in which negative beams of electrons, in the momentum range from 20 to 200 GeV/c, as well as pions and muons are available. The calorimeter test setup is schematically shown in Fig. 1a. Two scintillation counters S1 and S2 of dimensions

2.5×2.5 cm^2 and 3×3 cm^2 respectively were used to define the beam direction and time t_0 for the test run. In front of the calorimeter were placed a set of four veto scintillators covered with 6 mm thick Pb plates in order to reject those events in which the shower process starts upstream of the calorimeter. The veto counters define the beam spot size of 2×2 cm^2 for the calorimeter. Two Cathode Strip Chambers[9] (CSC) were used to locate the particles in the x-y direction on the face of the calorimeter The CSC positition resolution are nominally better 70μm.

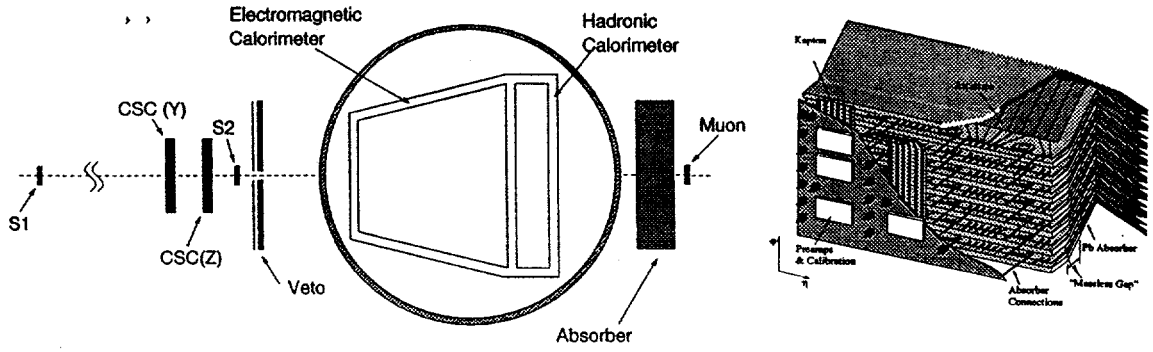

Fig. 1. a) Experimental setup for the test run. b) Isometric view of the calorimeter module.

2.1. The Calorimeter Module

The shape of the test calorimeter is a projective cylindrical wedge with a front face of dimensions 60×37.5 cm^2 and depth of 55 cm which corresponds to 25X_0 wih liquid krypton. An isometric view of the accordion showing the electrical connections, and internal electronics is shown in Fig. 1b. The absorber plates are made of 1.0 mm Pb plates sandwiched between two sheets of 0.2 mm stainless steel. Stainless steel provides both the mechanical strength as well as a better surface than lead. There is a nominal 2 mm liquid gap between the absorber and the electrode. A small hadronic module of an EST parallel plate design followed the electromagnetic module.

2.2. Readout Electronics

The readout chain used in the experiment is show in Fig. 2. Both the pre-amplifier and the calibration circuits are located as close as possible to the signal electrodes and are operated at cryogenic temperatures [10]. The high voltage connections to the electrodes are distributed over busses located on the electrode boards. The motherboard contains routing for all output signals, calibration signals, and low voltage power. Transmission lines of 50 Ω characteristic impedance terminated at both ends connect the preamplifier output to an intermediate amplifier and cable driver located on the exterior wall of the cryostat. The intermediate amplifier has a switchable voltage gain of 2 or 9 (the gain is fixed at 9 for the lower dynamic range front (strip) section

and for the hadronic section), and drives differentially a 100 Ω shielded twisted pair cable 35 meters long. The signals are received in the counting room by Variable Gain Amplifiers (VGA).

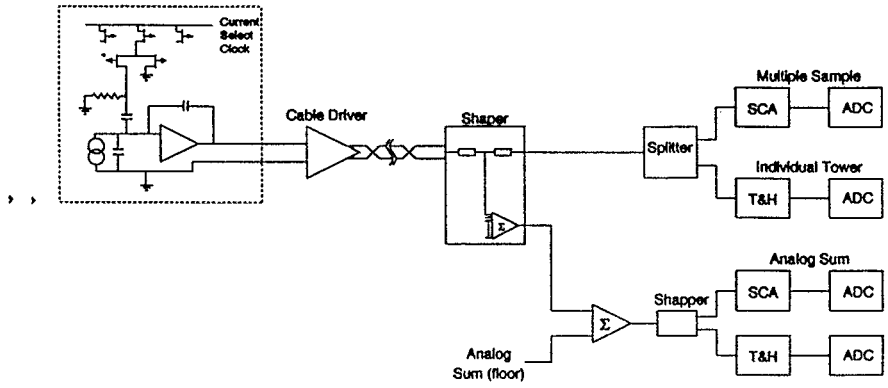

Fig. 2. Electronic readout chain.

The signals arriving at the VGA are split into two. One path takes the signal to a 40 ns, bipolar shaper/amplifier and the other path is input to a current sum used in the trigger. The most important control feature of the VGA is the adjustment of channel gain within a range of ±20% through a voltage-controlled capacitance in the amplifier. The voltage is set through a 12-bit DAC driven by a on-board microprocessor. This feature of the VGA, in combination with the calibration system discussed below, permits equalization of gains to a precision of a 0.2%. All shaped signals are fed into track and hold units and digitized by a 12-bit fastbus ADC.

A non-loading, high input impedance circuit ("High Impedance Pick-off") branches off some of the individual channels which together with the analog sums are sampled every 25 ns and stored in a switched capacitor array, thus simulating the mode of data acquisition likely to be employed at the LHC. A total of 32 samples per channel were kept for offline analysis. The status of the SCA readout is discussed by J. Parsons presentation in this conference.

One of the important advantages of liquid ionization calorimetry is stability and uniformity of response. In this test we used a calibration system developed at BNL that is based on the distribution of DC current to individually selected channels. The system thus permits the calibration of individual channels. With this technique an interchannel gain uniformity of better than 0.2% has been achieved.

2.3. Cryogenics and Purification System

A specially made bathtub surrounded the calorimeter modules with the goal of minimizing the amount of krypton required. The cryostat is the same as was used in our previous test in 1992[6]. The krypton was cooled and liquified using a liquid nitrogen heat exchanger at the top of the cryostat.

We used the same krypton as in 1992 but ran it through an Oxysorb filter before liquefying. We measured the stability of the signal and the lifetime of electrons in the krypton using a small ionization chamber and a ^{241}Am source (alpha cell) imersed in the same krypton as the calorimeter. Fig. 3a shows the response of this alpha cell as well as a curve resulting from the convolution of the associated electronics impulse response with the krypton current signal. From the calculation a drift velocity of 3.8 $mm/\mu s$ at the nominal voltage of 10KV was derived. The total charge that the source deposit in the alpha cell was measured several times each day during our two week run, no measureable change in the charge during this time was found to the 1% level. We emphasize that no special treatment of the materials that entered the cryostat other than alcohol cleaning was needed and there was no need to purify the krypton once it was liquified.

3. Experimental Results

3.1. Calorimeter Response

Fig. 3b displays the shaped signals from the calorimeter taken at different high voltage settings. As the applied high voltage is raised, the electron signal reaches a limiting value. This can be seen both in the pulse shape and in amplitude. In liquid krypton, however, the drift velocity is already large at very low voltages and even at 50 V a pulse with 30% of the maximum amplitude can be seen. The data we are reporting in this paper were taken at 2000 V.

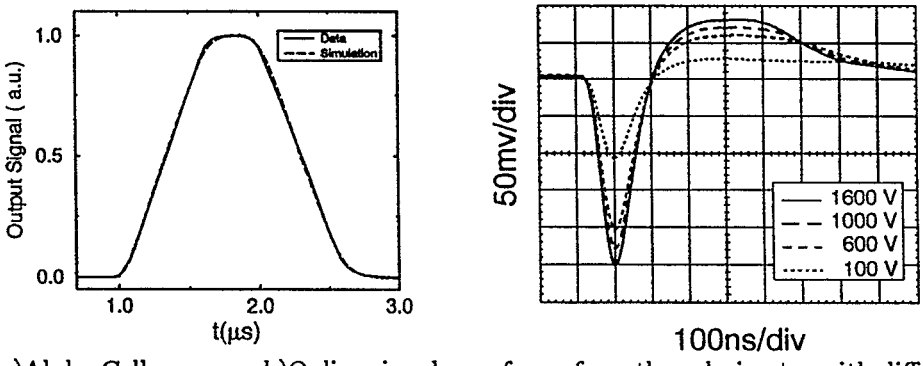

Fig. 3. a)Alpha Cell reponse. b)Online signal waveforms from the calorimeter with different voltage settings

3.2. Energy Resolution

To determine the energy resolution of the calorimeter, we define an active region to be a 6×6 tower configuration around the position of the incident particle. The energy was corrected for ϕ modulation, energy loss in the front of the calorimeter as well as energy leakage at the back. Minimal corrections are needed to compensate for the amount of energy deposited before the active part of the calorimeter, due to the presence of a passive massless gap. Using the corrected data, we show in Fig. 4a the energy spectrum obtained for 200 GeV electrons. The distribution of pedestal events are shown in the figures, and their width obtained from Gaussian fits are σ=240 MeV for 30 towers. Thus the equivalent noise for a single readout tower is 43 MeV/tower for the low-low gain setting. The rms value divided by the mean of the spectrum in Fig. 4a energy resolution of $5.5\%/\sqrt{E}$, after the noise contribution is subtracted in quadrature. There is no correction for the momentum spread of the beam

The fitting procedure was repeated for each of the eight beam momenta at which data were taken from 20 to 200GeV/c. In Fig. 4b, we show these data, along with a line fitted to the function

$$\frac{\sigma_E}{E} = a \oplus \frac{b}{\sqrt{E}}.$$

The fitted values of the parameters are a= (0.27±0.2)% and (b=0.055±0.004) $\sqrt{\text{GeV}}$.

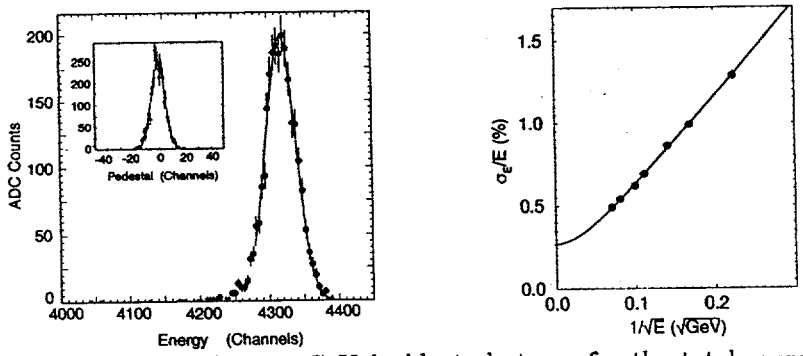

Fig. 4. a)Energy spectrum for 200 GeV incident electrons for the total energy sum. b)Energy Resolution as a function of $1./\sqrt{E}$

The linearity of the calorimeter response, over a range from 20 GeV to 200 GeV, is defined as the ratio of the fitted mean energy to the nominal beam energy. The relative deviations from a straight line as a function of beam momentum have been

measured and the system is found to be linear over this energy range to within 0.1%.

3.3. Energy resolution as a function of inactive material

In a realistic electromagnetic calorimeter for a collider experiement, inactive material in front of the active calorimeter is inevitable. In this test, the amount of inactive material in front of the active calorimeter is $1.2X_0$ in the regular setup. To study the calorimeter response to additional inactive material, lead plates of various thicknesses were placed immediately upstream of the cryostat. The total amount of inactive material varied from $1.2X_0$ to $5.2X_0$.

A 50 GeV electron beam was used in this study. The total observed energy is plotted as a function of total inactive material in Fig. 5a. The resolution is determined from energy distributions where weights for each longitudinal sections were optimized for each case. It is clear that the addition of innactive material of $2.0X_0$ thickness results in a non-recovarable energy resolution.

3.4. Position and Pointing resolution

The shower position is measured with the transverse segmentation of the calorimeter for each longitudinal section. In the front section, three strips centered around the one with highest energy are used in the position calculation, while in the towers, 3×3 towers centered around the tower with highest energy are used. Fits to the curves are then used to correct for the non-linear relation between the impact point and simple energy weighted position. The position resolution is the width of the difference between the chamber position and position measured by the calorimeter. The noise contribution to the position measurement is negligible at the energies under study.

Fig. 5b shows the position resolution as a function of the beam momentum for the strips and middle longitudinal segment. A fit of the form

$$\sigma = a/\sqrt{E} \oplus b$$

gives the parameters a=2.7 mm $GeV^{1/2}$,b=0.24 mm for the strips, and a=4.4 mm $GeV^{1/2}$ and b= 0.3 mm for the middle longitudinal segment.

Using the positions measured at the three different depths, the angle of the calorimeter shower is also measured. In this calculation the average shower centroid in the longitudinal direction for each longitudinal segment is assumed according to the Monte Carlo simulation. The θ angular resolution obtained can be parametrized as

$$\sigma_\theta = (41 \pm 0.4/\sqrt{E} \oplus 2.0) mrad$$

3.5. Response to Muons

The calorimeter muon response is displayed in Figures 6a. The muon energy was

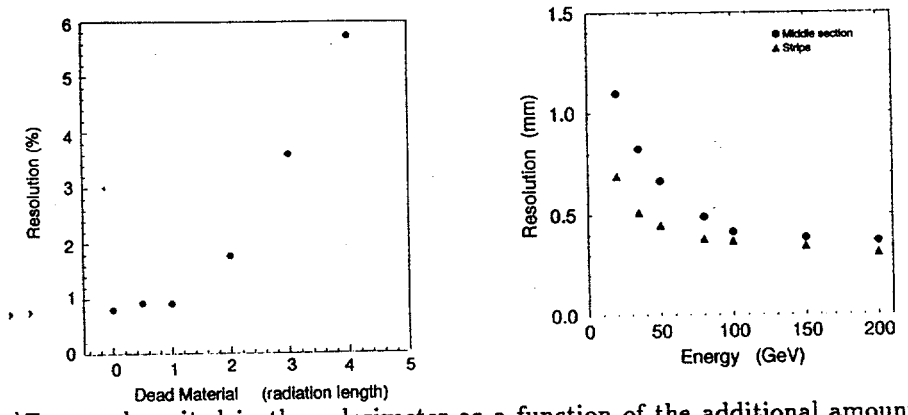

Fig. 5. a)Energy deposited in the calorimeter as a function of the additional amount of material infront of the calorimeter. b) Position resolution for the Strip section and Middle section.

defined as the energy deposited in a 2×1 tower geometry. The pedestal (in units of energy) is displayed along with the data and illustrates the signal to noise one can achive with this system.

The suppression of the response of an electromagnetic shower relative to that of a minimum ionizing particle is usually called the e/μ ratio, which we define as the ratio of the electron response to the muon response (peak) for a given amount of energy lost in the calorimeter. The muon total energy loss was computed using the GEANT simulation program. Using the linear response curve obtained in the electron runs, the electron response for the same amount of energy loss was calculated. The e/μ ratios for liquid krypton is 0.83 ± 0.01.

3.6. Timing Resolution

The timing performance of the calorimeter was measured by discriminating the shaped signal from the middle section analog sum. The discriminator used has been described earlier [5]. The timing was measured in a TDC which was started by the beam scintillators and stopped by the output of the constant fraction discriminator (CFD). The online information is corrected offline for difference in cable lengths using the algorithm of Ref [5]. The timing resolution achieved during the test for electrons of 120 GeV is 260 ps. This resolution was limited by the scintillator timing resolution of 190ps and largely by the shaper (second stage) noise.

3.7. Photon Data

In addition to the the electron data we have also taken data with a tagged photon beam. The energy of the photon were between 35-80 GeV depending on the setup. The analysis of the data is ongoing, in Fig. 6b we show a typical event dump where one can immediately see the advantages of the integrated preshower for γ/π^0 separation.

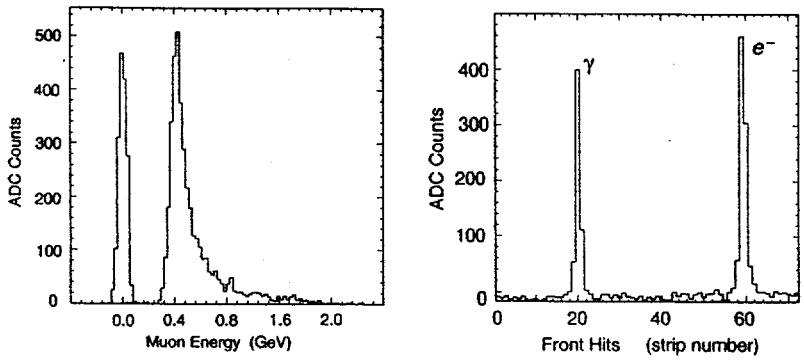

Fig. 6. a) Muon Energy deposition for the High High configuration. b) Event dump showing the energy profile of a photon and the electron from the tagged beam

The photon signal in the preshower is narrow and well separated from the noise. This will enable us to do a detailed shower shape analysis. General features of the data are in good agreement with the Monte Carlo (MC) but detailed analysis and comparison is now ongoing.

4. Discussion and Conclusion

We have tested sucessfully a projective liquid krypton accordion calorimeter with an integrated preshower. We found: i) The krypton signal was stable over the two weeks of the run, with no purification needed. ii) The energy resolution obtained was in good agreement with the MC expectation, showing that the accordion design can achive resolution below 6% with a very small constant term. iii)Pointing resolution of the order of 40 $mrad/\sqrt{E}$ can be obtained with an integrated preshower. iv) Preliminary result on the shower shape analysis of photons look very encouraging. v) Inactive material does not deteriorate the calorimeter response significantly below $2X_0$. vi) The passive massless gap in the absorber minimizes the need for correction as a function of longitudinal shower development.

5. Acknowledgments

Our design of the accordion electrode structure has relied on the pioneering work of the RD3 collaboration. We would like to thank the the many people at CERN who were more than helpful during the test. In particular we would like to thank the teams from RD3/ATLAS, NA48 who have given us special help during the run. We also acknowledge the loan of the krypton from the Budker Institute for Nuclear Physics.

This research was supported in part by the U.S. Department of Energy under

contract DE-AC02-76CH 00016. Part of this work is supported by the SSC closeout funds.

6. References

1. ATLAS, Conceptual design report
2. GEM experiment Technical Design Report, GEM TN-93-262 (1993) unpublished.
3. B. Aubert et al., Nucl. Inst. and Methods A309(1991)438.
4. B. Aubert et al., Nucl. Inst. and Methods A321(1992)467.
5. O. Benary et al., Nucl. Inst. and Methods, A344,(1994)78.
6. O. Benary et al., Nucl. Instr. and Methods, A344(1994)363
7. O. Benary et al., Nucl. Instr. and Methods, A350(1994)131
8. O. Benary et al., Nucl. Instr. and Methods, A349(1994)367
9. G. Bencze et al., BNL Report 60837, (1994) Nucl. Instr. and Methods (in Press)
10. V. Radeka and S. Rescia, Nucl. Inst. and Methods A265 (1988) 228